Design and Evaluation of Modular Gas and Wind Sensing Nodes for Static and Mobile Deployments

Wanting Jin, Emmanuel Droz, Alcherio Martinoli

***Abstract*— Static and mobile sensor nodes can be employed in gas monitoring tasks to detect gas leaks in an early stage and localize gas sources. Due to the intermittent nature of gas plumes and the slow dynamics of commonly used gas sensors, measuring gas concentrations accurately and timely poses significant challenges. These challenges are exacerbated when measurements are gathered while moving. Actively sniffing in the airflow, facilitated by actuators, holds the potential to improve the quality of measurements obtained by the sensor nodes. In this paper, we present the design of a small-scale, modular sensor node endowed with gas and wind sensing modalities. To assess the benefits of active sampling and the rationale behind this enhancement, comparisons among three different air sampling modes in both static and mobile settings are conducted. Our findings suggest that passive sampling can adequately capture the primary features of gas plumes given sufficient exposure and measuring time at each position. However, active sampling enhances the responsiveness of sensor nodes, enabling the detection of more detailed fluctuations in the gas concentration and thus alleviating spatial shifts in the sensor response induced by mobility effects.**

I. Introduction

Leakage of chemical gas poses a severe threat to humans and animals, as well as to the environment. In recent decades, notable advances have been made in sensors, embedded systems, and robotics, targeting chemical sensing [1]. Consequently, the application of robots and wireless sensor networks for olfaction has been steadily gaining momentum. Gas sensor nodes, operated under different mobility conditions, can effectively contribute to tasks such as Gas Source Localization (GSL) and Gas Distribution Mapping (GDM) [2]. Static sensor networks can be used to monitor gas concentration in the environment and detect gas leaks at an early stage [3]. Mobile sensor networks, typically leveraging mobile robotics technology, are used to search for the location of the gas source [4] and map the gas distribution [5], when leakage occurs.

Compared to radiation [6] or light [7] source localization problems, gas dispersion is a complex phenomenon, dominated by airflow advection and influenced by turbulent and molecular diffusion [8]. Consequently, the gas plume is intermittent and chaotic [9]; in other words, the gas field is not continuous and isotropic, and the gas concentration at a given point in the gas plume is dynamic and fluctuating. Gas concentration can be measured using remote sensing, for instance through Tunable Diode Laser Absorption Spectroscopy (TDLAS) sensors [10], or in-situ sensing, leveraging technologies such as Metal-Oxide (MOX) [11] and Photo-Ionization Detection (PID) [12]. While TDLAS sensors provide measurements remotely without being affected by sensor mobility, they tend to be too bulky for platforms affected by severe restrictions in sensing payload. In addition, TDLAS sensors report gas concentration as an integral result over the entire beam path, making the detailed distribution of the gas plume difficult to access. In contrast, PID and MOX sensors can capture the detailed changes inside gas plumes but require direct exposure of the sensor's sensitive layer to gas molecules. In addition, PID and MOX sensors suffer from low selectivity and a relatively long reaction and recovery time, which limit their overall real-time performance in motion.

When employing in-situ sensors for gas sensing tasks, accurately measuring gas concentrations becomes challenging due to the patchiness of the plume and the slow dynamics of the sensors. If measurements happen while moving, these challenges are exacerbated by a reduced contact time between the gas molecules and the sensor's sensitive layer [13], along with additional disturbances to the gas plume due to the movement of the sensing platform. An appropriate mechatronic design of the sampling system can help mitigate such issues. Sampling systems can be classified as passive and active. A passive sampling system exposes the sensor directly to the target gas and relies on the background airflow to bring the gas molecules to the sensor. An active sampling system, on the other hand, uses an actuator to actively sniff or flush the gas molecules and expose them to the sensor. In [14], a fan-based sniffer was used in a stereo electronic nose and tested in a static configuration, maintaining a constant relative distance between the sensor and the gas source. Active sniffing was found to reduce the recovery time of the MOX sensor by a factor of two. However, the experiments were not conducted in precisely controlled settings. In another study [15], pump- and fan-based sniffers were compared in a mobile air quality monitoring sensor network. The study found that a raised-inlet pump-based sniffer demonstrated the capability to enhance the signal-to-noise ratio, thereby indirectly improving the sensor's dynamic response. The effectiveness of active sampling with an axial fan and a deconvolution technique was investigated in [16] to mitigate the slow dynamics of air quality sensor nodes. The study concluded that active sampling offers advantages for feature

The authors are with the Distributed Intelligent Systems and Algorithms Laboratory, School of Architecture, Civil and Environmental Engineering, École Polytechnique Fédérale de Lausanne (EPFL), 1015 Lausanne, Switzerland. This work was partially funded by the Swiss National Science Foundation under grant 200020_175809. Additional information about the research can be found here: https://www.epfl.ch/labs/disal/research/gassensingstructure/

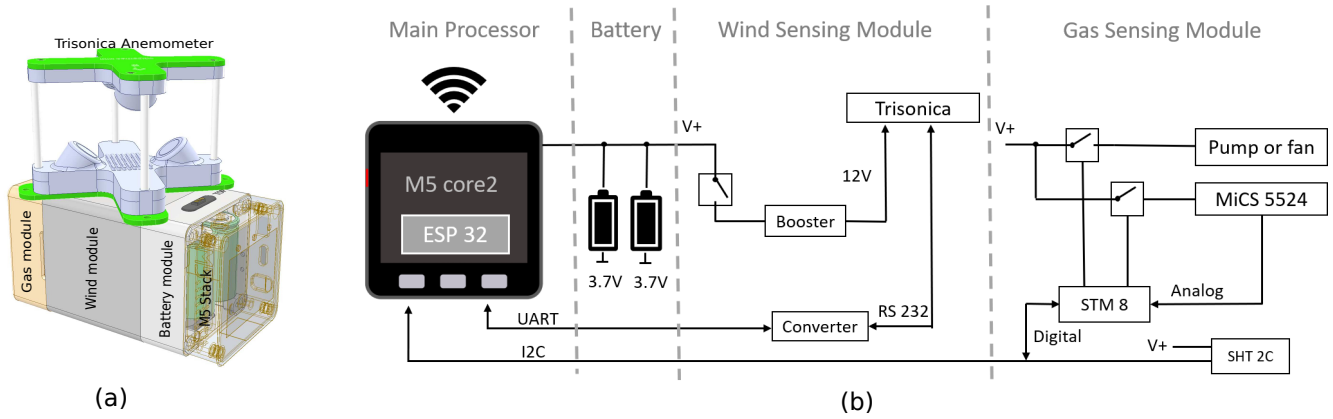

Fig. 1: (a) 3D Sketch of the modular sensor node; (b) Electrical diagram of the sensor node.

localization, particularly with high speed movement of the sensing platform. Consequently, previous research suggests that active sampling has the potential to enhance the sensing quality. However, the underlying reasons for its effectiveness and applicability across different sensor mobility remain unclear.

In our research, we are interested in portable devices enabling distributed static or mobile gas sensing, typically indoors. Given the unconventional application scenarios, no commercially available sensor nodes meet our requirements. Therefore, in this paper, we present the design and a systematic evaluation of our modular sensor nodes, which in addition to combining wind and gas sensing modules, can be endowed with passive and active gas sampling solutions. In particular, this paper makes the following contributions.

- Section II - Modular design of a sensor node endowed with gas and wind sensing, flexible energy reservoir, wireless communication, and extended computational capabilities (e.g., comfortable programmability, data visualization).
- Section III - Mechatronics design of active gas sampling solutions with fans and pumps. Systematic tests of active sensing in different controlled environments, namely in a gas chamber and in a wind tunnel, in presence of different mobility patterns.
- Section IV - Benchmarking of the performance of different sampling solutions with the sensor dynamic property and the sensitivity to the presence/absence of the gas.
- Section V - Design considerations about various trade-offs between sensing quality and power consumption as a function of the node mobility characterizing application scenarios.

II. Sensor Node Design

We have designed wireless sensor nodes equipped with wind and gas sensing capabilities, WiFi connectivity, and standalone battery packs. The design facilitates easy deployments in experimental fields and ensures reasonable energetic autonomy, which can be extended with larger battery packs, if required. To enhance the versatility of sensor nodes and allow deployment of the sensor network in a heterogeneous configuration, the battery pack, the gas sensing module and the wind sensing module are independently developed and connected in a "sandwich" architecture, as shown in Figure 1 (a). The detailed development of each module is explained in the following subsections.

A. Main Processor

The M5Stack Core2[1] has been selected as the core computational board for the sensor node. It uses the ESP32 model D0WDQ6-V3 as its microcontroller unit. Its compact design, touch screen interface, built-in WiFi connectivity, and support for UART, I2C, SPI, and GPIO functions for peripheral connections make it highly suitable and easily extendable for our project. The gas sensing module is connected to the M5Stack over I2C, while the wind sensing module uses the UART interface. The M5Stack controls the working mode of each module and displays the measurements on the embedded screen, with the electrical diagram presented in Figure 1 (b). MQTT has been chosen as the communication protocol between the sensor node and an external server, given its stability, lightweight nature, and extensibility.

B. Battery Pack

The battery pack has been designed to expand the battery capacity of the sensor node. It is seamlessly integrated with the M5Stack via the same input/output configuration bus, simplifying the connection of additional modules to the main computational unit. Each battery pack contains two rechargeable single cell (3.7 V) Li-ion batteries with a capacity of 1200 mAh. This capacity of the sensor node can be expanded by connecting multiple battery packs.

C. Wind Sensing Module

Wind measurements play a crucial role in gas sensing, especially in GSL, as they provide information on the direction in which gas particles travel before reaching the measurement points. To enable this sensing ability, we have integrated an off-the-shelf wind sensor, the Trisonica Mini from Li-COR[2], into the wind sensing module. This compact (9.1 cm x 9.1

[1]https://docs.m5stack.com/en/core/core2
[2]https://anemoment.com/

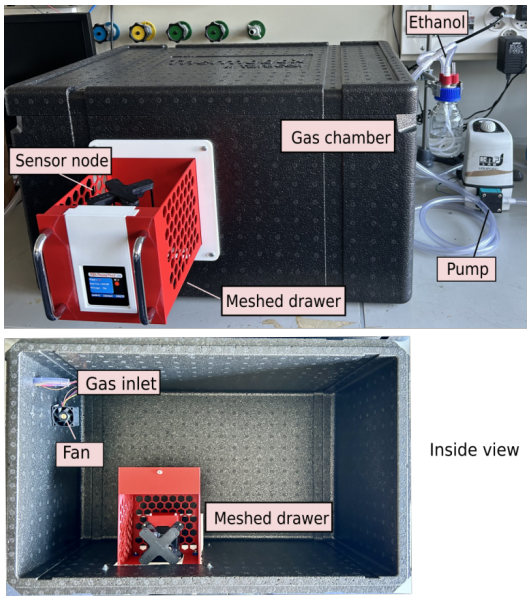

Fig. 2: Gas chamber test setup.

cm x 5.2 cm), lightweight (50 g) sensor leverages ultrasonic technology, which can sample airflow up to 40 Hz.

D. Gas Sensing Module

MOX sensors are the predominately employed gas sensor in embedded systems [4], [17]–[21], given their compact size, low cost, relatively fast response time, and high sensitivity [11].

1) MOX sensor selection: MOX sensors are hindered by a relatively long recovery time, which limits their real-time responsiveness during motion. However, data regarding dynamic properties are typically unavailable in sensor datasheets since such properties are not essential in conventional applications for which this sensing technology has been designed. Therefore, it is crucial to perform the characterization of such properties for achieving an informed sensor selection. To do so, the sensor needs to be exposed to the target gas and clean air in a controlled manner. Traditionally, this is achieved by using a vacuum chamber and controlling the release of the target gas via an electrical valve. However, such devices are expensive to manufacture and difficult to maintain. Alternatively, we have employed a 3D-printed drawer mechanism to control the exposure of the sensor. This method simply involves inserting and withdrawing the drawer containing the sensor module, making it both cost-effective to produce and easy to maintain. The setup for the gas chamber test is shown in Figure 2. The gas is injected into the chamber through a pump that mixes ethanol with air. The sensor node is placed inside a drawer with a meshed enclosure to facilitate air exchange. When the drawer is inserted into the chamber, the sensor is exposed to the gas, and when it is withdrawn, the sensor encounters clean air. A fan mounted at the bottom of the chamber ensures a uniform distribution of the gas. We compare the performance of three MOX sensors, the MiCS 5524, the

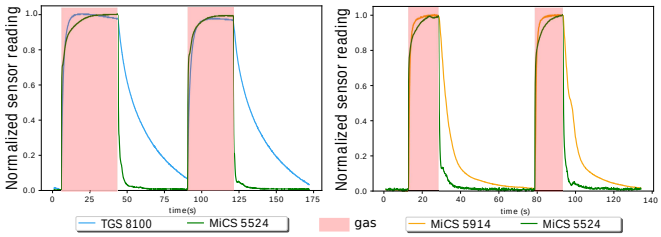

Fig. 3: Chamber test results of sensor dynamic properties.

MiCS 5914 from SGX SensorTech[3], and the TGS 8100, from FIGARO[4]. As illustrated in Figure 3, the MiCS 5524 exhibits a slightly longer reaction time but a significantly shorter recovery time compared to the other two sensors, thus it has been selected as the gas sensor for our project. We have designed a dedicated Printed Circuit Board (PCB) for the analog/digital conversion and communication between the gas sensing module and the main processor. This module samples the MOX sensor at 10 Hz.

2) Sensor reading calibration: The MOX sensor comprises a heated metal oxide surface whose electrical resistance (R_s) varies in response to the oxygen ions present on its surface. To measure R_s, a simple voltage divider is leveraged, characterized by the supply voltage V_T and a loading resistor R_L. The voltage measured across the loading resistor V_L is used as the sensor output. R_s can be calculated by applying the voltage divider equation:

$$R_s = R_L * \frac{V_T - V_L}{V_L} \quad (1)$$

The logarithm of the ratio between sensor resistance R_s and its resistance when exposed to clean air R_0 demonstrates a linear correlation with the logarithm of the gas concentration. The linear function varies based on the type of gas being detected. Given that the gas composition is typically a mixture from the surrounding environment, determining the absolute concentration of a specific gas is not practical. Instead, the ratio between the R_0 and R_s is utilized as a measure of relative gas concentration [22]. To address the potential drifts in the sensor baseline caused by the variation in humidity, temperature, and sensor age [23], R_0 is recalculated before each experimental trial as a calibration routine.

III. Sampling Modes

Active sampling can potentially improve the measurement quality of the gas sensing module by actively sniffing the airflow to increase the chance of detection of gas patches.

A. Mechatronic Design

To study the effect of active sampling, three different solutions have been developed, as shown in Figure 4.

- *Passive Sampling:* exposes the sensor's sensitive layer directly to the field. To prevent the accumulation of gas inside the node volume and damages caused by potential collision with external objects, a shield with a meshed window and four septums has been designed.

[3]https://www.sgxsensortech.com/
[4]https://www.figarosensor.com/

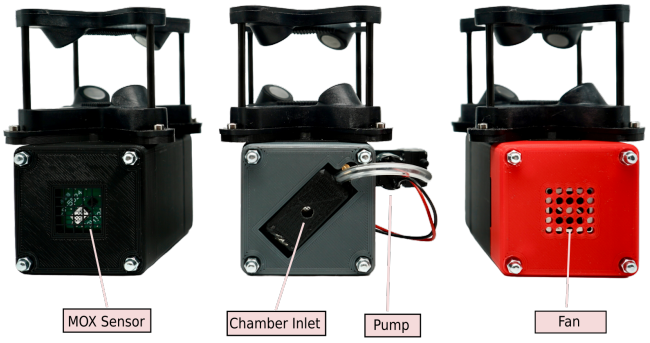

Fig. 4: Passive and active sampling solutions.

- *Pump-based Active Sampling:* employs a sensor chamber with the outlet connected to an air pump (micro diaphragm gas pump NMP05KPDC-S from KNF[5]), and the input opened to the field. The pump sucks air in and generates an airflow vertical to the sensor's surface, which is controlled by a dedicated sensor chamber, with a circular inlet of 0.5 mm, located on top of the sensor surface. The pump works with 5V input and the generated inlet airflow speed is 0.34 m/s.
- *Fan-based Active Sampling:* employs a design similar to passive sampling, with a microaxial fan (1804 fan from Yuanfanpower[6], with a radius of 15 mm) fixed between the meshed window and the sensor. The fan sucks air in and delivers it to the sensor's surface vertically. The fan can work under two input voltage conditions, 5 V and 3.3V. We choose to supply it with 5V input, under which the airflow speed is 2.408 m/s.

B. Test Setups

To assess the effectiveness of active sampling in environments characterized by varying degrees of turbulence and investigate the influence of mobility on sensing quality, experiments were carried out in two different setups: the gas chamber illustrated in Section II and a wind tunnel.

In the chamber test, the sensor node's dynamic properties were examined using the previously introduced gas sensor chamber. This test reproduced a static deployment in an environment where the gas is uniformly distributed and its concentration remains constant.

In real-world deployments, reaching constant concentration is uncommon due to fluctuations caused by advection and turbulence of the airflow. Systematic tests were conducted in a wind tunnel to evaluate the sensing quality of the node under realistic airflow conditions. The experimental setup in the wind tunnel is illustrated in Figure 5. The wind tunnel has a volume usable of 18 m × 4 m × 1.9 m and allows for the execution of experiments in a repeatable manner, under a specific wind speed. The gas source was represented by an electric pump vaporizing ethanol. A 3-axis traversing system was leveraged to enable 3D movements of the sensor node mounted on top of it. The source was

[5]https://knf.com/en/ch
[6]https://www.yunfanpower.com/

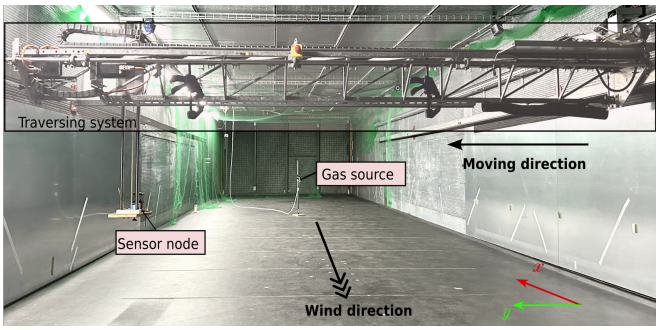

Fig. 5: Wind tunnel experiment setup.

placed upwind in the middle of the wind tunnel. The wind blew along the x-axis at a constant speed of 0.75 m/s in all experiments. In each experiment, the sensor traversed the plume by moving along the y-axis, starting initially outside the plume, entering it, and subsequently exiting it. Three different relative distances between the source and the traversing system along the x-axis were considered, namely 3 m, 5 m, and 7 m. Each experimental trial was repeated five times.

To evaluate the impact of active sampling under different mobility conditions, experiments were conducted using two different motion patterns:

1) Stop-and-sense strategy: For each run, the traversing system stopped at each sample position, waited there for 3 s to allow the sensor to reach the steady state, and the gas concentration was measured during 5 s. The spatial interval between the sample points along the y-axis was 0.156 m.

2) Sense-in-motion strategy: The traversing system moved continuously while the sensor node was gathering gas measurements. Two different moving speeds were tested, 0.18 m/s and 0.35m/s, which both represent typical moving speeds of one of our small-scale indoor mobile robots.

IV. Results

Two matrices are introduced to evaluate the performance of active versus passive sampling under varying degrees of dynamics.

1) Reaction and recovery time: In steady environments (chamber test), the reaction (t_{rise}) and recovery (t_{decay}) time of the gas sensing module are measured to evaluate its dynamic properties. Reaction time refers to the duration it takes for the sensor output to reach 90% of the steady-state value when exposed to gas; recovery time refers to the duration it takes for the sensor output to return to 10% of the steady-state value when exposed to clean air.

2) Gas hit event: In environments characterized by significant airflow (wind tunnel test), fluctuating gas concentrations within the plume prevent the sensor from reaching a steady state as in the case of the chamber test. In addition, while sensing in motion, only instantaneous variations in the gas concentration can be measured. Thus, the magnitude of the sensor response is less accurate and varies across different runs. Under these conditions, the detection of gas hit events (relative changes in sensor readings) proves to be more informative and is widely used for the GSL problems [24] [25]

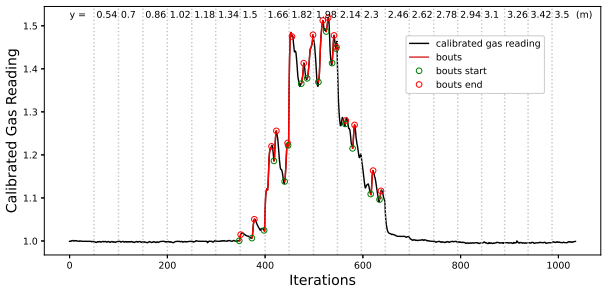

Fig. 6: The Bouts detections on the calibrated gas reading in a stop-and-sense scan with fan-based active sampling (raw data shown in black).

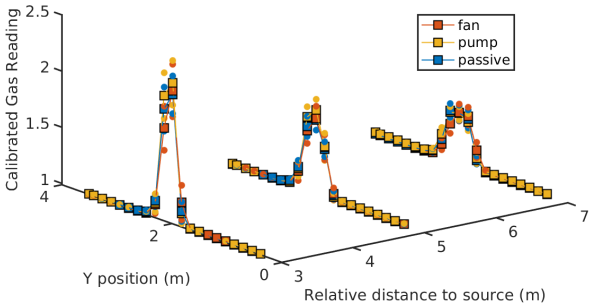

Fig. 7: Comparison of scans with the stop-and-sense strategy across different sampling modes at different distances from the source.

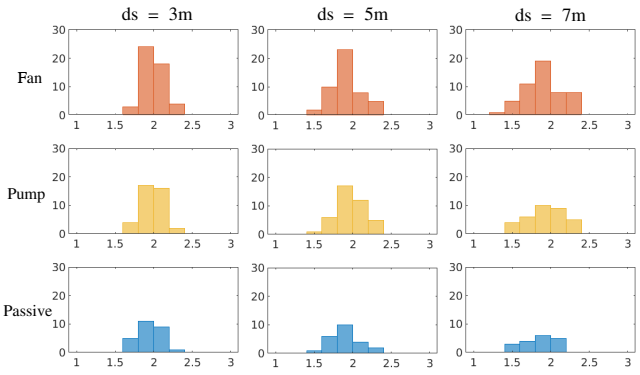

Fig. 8: Histogram of the bouts numbers as a function of the sampling position on the y-axis expressed in meters.

[20]. Declaring gas hit events based on predefined thresholds might be delayed due to the slow dynamics of MOX sensors. Instead, an algorithm leveraging MOX sensors' ability to extract rapidly fluctuating gas plume features, referred to as 'bouts', was proposed in [26]. These bouts, extracted from the rising edges of smoothed MOX sensor readings, may indicate the contact between the sensor and gas patches in the plume. Bouts' frequency correlates with the proximity to the gas source, with closer positions exhibiting higher intermittency in gas concentration, thus yielding higher number of detected bouts. To extract bouts, raw sensor readings are initially smoothed via an Exponentially Weighted Moving Average (EWMA) filter. Subsequently, the derivative of smoothed readings is computed and further smoothed with the same EWMA filter. Finally, the positive derivative values are extracted to identify the rising edge of the smoothed sensor readings. For implementation purposes, we adapted the code used in [22]. An illustration of bouts extracted for the stop-and-sense strategy is shown in Figure 6, with the black lines showing the raw data and the red lines showing the bouts in the raw signal, and green and red circles indicating the starts and ends of bouts, respectively.

A. Gas Chamber Experiments

The sensor node demonstrates comparable reaction and recovery times across various sampling modes. Notably, the chamber tests did not reveal any significant enhancement in the sensor node's dynamic properties with the employment of active sampling. This observation could be attributed to the steady and uniform distribution of gas/clean air within the chamber and the surrounding environment.

B. Wind Tunnel Experiments

Results of gas scans across various sampling solutions under different mobility patterns are analyzed.

1) Stop-and-sense: Gas scan results with the stop-and-sense strategy at different relative distances from the source (d_s = 3 m, 5 m, 7 m) are depicted in Figure 7. To improve the readability of the plot, each curve aggregates the results of five runs conducted with identical test configurations. The squares represent the average values, while the solid circles show the standard deviation bounds of all the measurements gathered at each sampling point. Note that the significant variance arises from the intermittent nature of the gas plume rather than the discrepancies across different runs. As evident in Figure 7, as the proximity to the source increases, the plume narrows, and the gas concentration rises. Across the three different sampling modes, the gas scan results demonstrate consistent trends in both magnitude and distribution. Under the same test conditions and the same strategy, the histograms of the detected bouts are shown in Figure 8. This representation of bouts reveals a similar distribution across different sampling modes, with the highest number of bouts detected close at the center of the channel, with source position and the sample point aligned on the y-axis. However, active sampling modes detect significantly more bouts in general, with the fan-based solution performing better than the pump-based one, indicating enhanced sensitivity to rapid fluctuations in the gas plume. In conclusion, with sufficient exposure and sampling time at each point, both passive and active sampling solutions capture similar characteristics of the gas plume. Active sampling modes excel in capturing the finer intermittency of the plume.

2) Sense-in-motion: During sensing in motion, as depicted in Figure 9, results indicate lower consistency across various runs compared to the stop-and-sense strategy. Additionally, the response curves show spatial shifts and magnitude decrements. These observations can be attributed to the slow dynamics of the sensor and the reduced contact

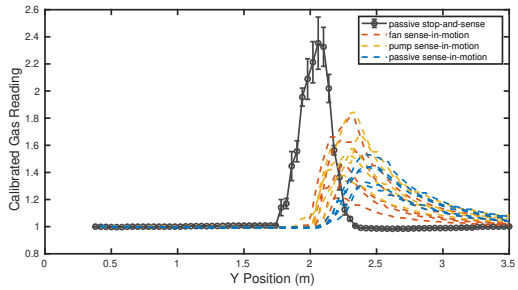

Fig. 9: Comparison of stop-and-sense and sense-in-motion (traversing system's speed of 0.35 m/s) strategies at a distance of 3 m from the source.

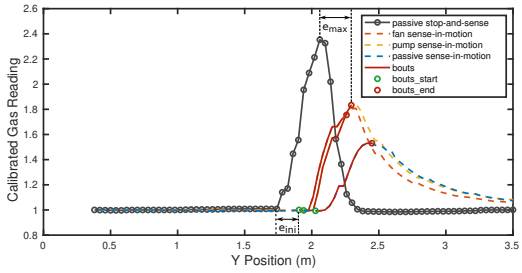

Fig. 10: Bout detections in sense-in-motion scans (traversing system's speed of 0.35 m/s) and the illustration of the shift in the initial response e_{ini} and the maximal response e_{max} position.

time between the gas molecules and the sensor's sensitive layer. While it may be impractical to directly compare the magnitude of the sensor responses across different sampling modes, we can still observe that active sampling enables the detection of gas at an earlier stage. Regarding the bouts detection, as illustrated in Figure 10, only a small number of bouts are extracted in the case of sense-in-motion. This is attributed to the limited sampling at each point and the smoothing effect (equal to a low pass filter) of mobility on the gas sensor response. In this instance, the bouts may not capture the actual intermittency within the gas plume. Still, they could indicate the position where the sensing module begins to detect the presence of gas, and that where the maximal response of the gas is reached. To assess the timeliness of the sensing module response to the presence of the gas, we utilize the scan results obtained with the stop-and-sense strategy and passive sampling with a spatial resolution of 0.04 m in the y-axis, as the ground truth for gas detection. The difference between the position of the rising point in the stop-and-sense scan and that where the first significant bout starts in the sense-in-motion scan represents the shift of the initial gas response position, denoted as e_{ini}. In addition, the difference between the position of the maximal response in the stop-and-sense scan and that where the last significant bout ends in the sense-in-motion scan represents the shift of the maximal gas response position, denoted as e_{max}. The definitions of e_{ini} and e_{max} are illustrated in Figure 10, with the result shown in Figure 11, where smaller values indicate a more prompt reaction to the presence of gas molecules.

The results indicate that, with passive sampling, the spatial shifts between the sensor reading response and the presence/absence of gas increases with higher moving speeds. This phenomenon arises from the increased travel distance during the sensor's reaction time and the reduced contact time between the gas stimulus/clean air and the sensor. These shifts can be partially compensated through an active sampling mechanism, with the fan-based approach generally outperforming the pump-based solution in most scenarios. This result can be attributed to the fact that actively sniffing in the airflow increases the chance of the sensor coming in contact with gas/clean air molecules. This effect is not observed in steady environments (as seen in the chamber experiments), where the gas/clean air is uniformly distributed. However, in wind tunnel settings, the significant airflow amplifies the patchiness and intermittency of the gas plume. Therefore, actively sniffing in the airflow partially works around the intrinsic patchiness of the plume by increasing the exposure volume reaching the sensor. While moving out of the gas plume, active sampling helps flush out the remaining gas molecules on the sensor surface, thus speeding up the recovering phase of the sensor. However, with slower moving speeds and greater distances from the source, the shift observed with passive sampling is less pronounced compared to other conditions, sometimes even reaching lower shifts than those obtained with active sampling mechanisms.

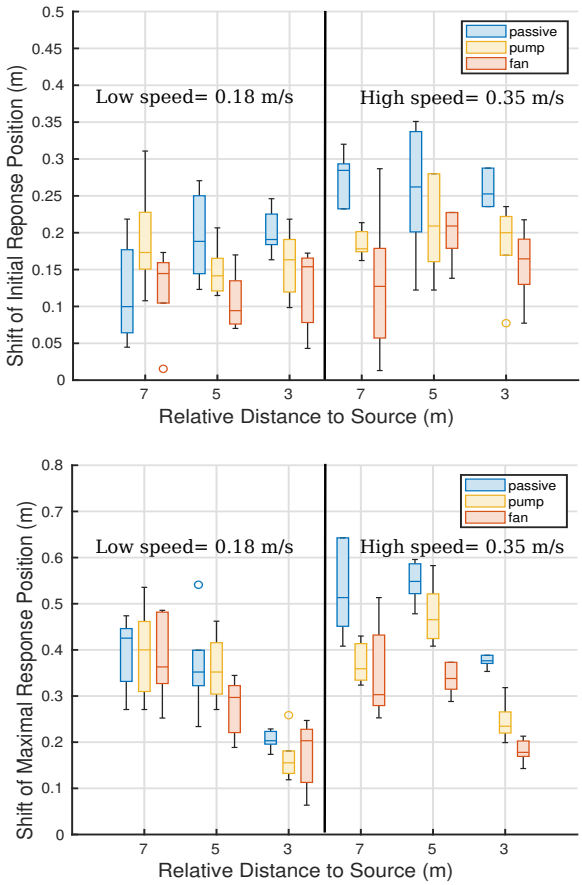

Fig. 11: Shift of initial and maximal response positions

V. Energy Consumption And Deployment Optimization

The aggregated and averaged power consumption for the gas sensing, WiFi communication, and M5Stack-based computation modules is about 330 mW. The Trisonica Mini wind sensor consumes 400 mW at the maximal sampling rate (40 Hz). Concerning the two active sampling solutions, the fan consumes 225 mW and the pump consumes 700 mW. The battery life of our modular sensor node with different operational modes is listed in Table I. In practical deployments, the stop-and-sense reflects the scenarios where the sensor node remains stationary throughout the mission or when a mobile sensor node is engaged in tasks demanding high resolution and measurement quality. Conversely, the sense-in-motion strategy is commonly employed with mobile sensor nodes when tasks are time-sensitive, and spatial sampling coverage is a key consideration. In the context of a static sensor network, power consumption plays a crucial role in ensuring the long-term functionality of the sensor node. With sufficient exposure time at each point, passive sampling proves adequate for capturing sufficient details of relative gas concentration and its temporal fluctuation. In contrast, for mobile sensor networks, especially those based on controllable mobility such as robotic assets, the power consumed for locomotion tends to be more significant than that required for sensing, therefore rendering active sampling mechanisms easily affordable. In scenarios involving a stop-and-sense approach for mobile sensing, a passive sampling mode may suffice if the time to accomplish the mission is less critical than the gas reading accuracy. However, during sense-in-motion operation, active sampling can be implemented to increase the reactivity in gas sensing, as illustrated by the results reported above.

In our design, the fan-based active sampling mode outperforms the pump-based one in terms of both sensor response time and power consumption. This fact can be attributed to the high efficiency of a fan in generating a larger airflow with less power. However, the pump-based sampling mode might offer a more robust solution, for instance in a dusty environment. Additionally, the pump-based solution provides greater flexibility in choosing the placement of the inlet (sampling point). Despite the significant difference in the generated airflow, the sensing modules do not show a large responsiveness difference.

Operation mode	Battery life(h)
Basic Operation Mode (M5Stack + gas module + MQTT)	26.9
Full Sensing Mode (Basic Operation Mode + wind module)	12.16
Active Gas Sensing With Fan (Basic Operation Mode + fan)	16.0
Active Gas Sensing With Pump (Basic Operation Mode + pump)	8.6

TABLE I: Battery life of different operation mode.

VI. Conclusion and outlook

In this study, we have presented the modular design of a compact wireless device equipped with gas and wind sensing capabilities. A customized gas chamber setup was designed to assess the dynamic properties of the gas sensing module in a controlled and steady environment. Additionally, we have investigated active gas sampling solutions to counteract the effects of the patchy nature of gas plumes and the slow dynamics of MOX sensors, thereby enhancing sensing quality. In particular, we systematically evaluated three sampling modes (passive, fan-based, and pump-based active sampling) in both chamber and wind tunnel tests. Our findings indicate that, while active sampling has a minimal impact on sensor dynamic properties in static deployment, it demonstrates the ability to enhance sensor responsiveness in more dynamic conditions. We suggest that, in scenarios involving static sensor networks, where sensor nodes have ample exposure to gas and energy consumption is a critical concern for long-term monitoring, a passive sampling approach is adequate to capture the primary characteristics of the gas plume. Conversely, in mobile sensor networks employing sense-in-motion techniques, active sampling proves valuable for capturing finer details of the plume and partially mitigating spatial shifts in the sensor response induced by mobility effects.

This study offers a reasonably comprehensive comparison between passive and active sensing solutions across various mobility patterns. Several mechatronics design choices remain open for further optimization. For example, further optimization of the size and shape of inlets for active sensing solutions through fluid dynamic simulation can be explored. Additionally, a deeper investigation of the relationship between sampling regime (e.g., airflow speed) and mobility pattern (e.g., moving speed) should be carried out. Potentially, a simple control law could be defined to optimize power consumption related to sampling under varying mobility conditions.

References

[1] L. Cheng, Q.-H. Meng, A. J. Lilienthal, and P.-F. Qi, "Development of compact electronic noses: a review," *Measurement Science and Technology*, vol. 32, no. 6, p. 062002, June 2021. [Online]. Available: https://iopscience.iop.org/article/10.1088/1361-6501/abef3b

[2] A. Marjovi and L. Marques, "Optimal spatial formation of swarm robotic gas sensors in odor plume finding," *Autonomous Robots*, vol. 35, no. 2-3, pp. 93–109, Oct. 2013. [Online]. Available: http://link.springer.com/10.1007/s10514-013-9336-1

[3] K. A. Klise, B. L. Nicholson, C. D. Laird, A. P. Ravikumar, and A. R. Brandt, "Sensor Placement Optimization Software Applied to Site-Scale Methane-Emissions Monitoring," *Journal of Environmental Engineering*, vol. 146, no. 7, p. 04020054, July 2020. [Online]. Available: https://ascelibrary.org/doi/10.1061/%28ASCE%29EE.1943-7870.0001737

[4] W. Jin, F. Rahbar, C. Ercolani, and A. Martinoli, "Towards Efficient Gas Leak Detection in Built Environments: Data-Driven Plume Modeling for Gas Sensing Robots," in *IEEE International Conference on Robotics and Automation*, London, United Kingdom, May 2023, pp. 7749–7755. [Online]. Available: https://ieeexplore.ieee.org/document/10160816/

[5] C. Ercolani, W. Jin, and A. Martinoli, "3D Gas Sensing with Multiple Nano Aerial Vehicles: Interference Analysis, Algorithms and Experimental Validation," *Sensors*, vol. 23, no. 20, p. 8512, Oct. 2023. [Online]. Available: https://www.mdpi.com/1424-8220/23/20/8512

[6] H. Zhu, H. Bai, P. Ding, J. Zhang, D. Wu, Z. Du, and W. Wang, "Dual-stage planner for autonomous radioactive source localization in unknown environments," *Robotics and Autonomous Systems*, vol. 172, p. 104603, Feb. 2024. [Online]. Available: https://linkinghub.elsevier.com/retrieve/pii/S0921889023002427

[7] W. C. Evans, D. Dias, S. Roelofsen, and A. Martinoli, "Environmental field estimation with hybrid-mobility sensor networks," in *IEEE International Conference on Robotics and Automation*, Stockholm, May 2016, pp. 5301–5308. [Online]. Available: http://ieeexplore.ieee.org/document/7487741/

[8] M. Rossi and D. Brunelli, "Gas Sensing on Unmanned Vehicles: Challenges and Opportunities," in *New Generation of CAS (NGCAS)*, Genova, Italy, Sept. 2017, pp. 117–120. [Online]. Available: http://ieeexplore.ieee.org/document/8052283/

[9] N. Holmes and L. Morawska, "A review of dispersion modelling and its application to the dispersion of particles: An overview of different dispersion models available," *Atmospheric Environment*, vol. 40, no. 30, pp. 5902–5928, Sept. 2006. [Online]. Available: https://linkinghub.elsevier.com/retrieve/pii/S1352231006006339

[10] P. P. Neumann, H. Kohlhoff, D. Hüllmann, A. J. Lilienthal, and M. Kluge, "Bringing mobile robot olfaction to the next dimension—UAV-based remote sensing of gas clouds and source localization," in *IEEE International Conference on Robotics and Automation*, 2017, pp. 3910–3916.

[11] C. Wang, L. Yin, L. Zhang, D. Xiang, and R. Gao, "Metal Oxide Gas Sensors: Sensitivity and Influencing Factors," *Sensors*, vol. 10, no. 3, pp. 2088–2106, Mar. 2010. [Online]. Available: http://www.mdpi.com/1424-8220/10/3/2088

[12] T. Wiedemann, D. Shutin, and A. J. Lilienthal, "Experimental Validation of Domain Knowledge Assisted Robotic Exploration and Source Localization," in *IEEE International Conference on Autonomous Systems*, Montreal, QC, Canada, Aug. 2021, pp. 1–5. [Online]. Available: https://ieeexplore.ieee.org/document/9551145/

[13] J. G. Monroy and J. Gonzalez-Jimenez, "Gas classification in motion: An experimental analysis," *Sensors and Actuators B: Chemical*, vol. 240, pp. 1205–1215, Mar. 2017. [Online]. Available: https://linkinghub.elsevier.com/retrieve/pii/S0925400516314307

[14] A. Lilienthal and T. Duckett, "A stereo electronic nose for a mobile inspection robot," in *1st International Workshop on Robotic Sensing, 2003. ROSE' 03.* Orebo, Sweden: IEEE, 2003, p. 6. [Online]. Available: http://ieeexplore.ieee.org/document/1218709/

[15] A. Arfire, A. Marjovi, and A. Martinoli, "Enhancing measurement quality through active sampling in mobile air quality monitoring sensor networks," in *IEEE International Conference on Advanced Intelligent Mechatronics*, Banff, AB, Canada, July 2016, pp. 1022–1027. [Online]. Available: http://ieeexplore.ieee.org/document/7576904/

[16] A. Arfire, A. Marjovi, and A. Martinoli, "Mitigating slow dynamics of low-cost chemical sensors for mobile air quality monitoring sensor networks," in *Proceedings of the 2016 International Conference on Embedded Wireless Systems and Networks*, 2016, pp. 159–167.

[17] C. Ercolani and A. Martinoli, "3D Odor Source Localization using a Micro Aerial Vehicle: System Design and Performance Evaluation," in *IEEE/RSJ International Conference on Intelligent Robots and Systems*, Las Vegas, NV, USA, Oct. 2020, pp. 6194–6200. [Online]. Available: https://ieeexplore.ieee.org/document/9341501/

[18] F. Rahbar, A. Marjovi, and A. Martinoli, "Design and Performance Evaluation of an Algorithm Based on Source Term Estimation for Odor Source Localization," *Sensors*, vol. 19, no. 3, p. 656, Feb. 2019.

[19] S. Shigaki, M. Fikri, and D. Kurabayashi, "Design and experimental evaluation of an odor sensing method for a pocket-sized quadcopter," *Sensors*, vol. 18, no. 11, p. 3720, 2018. [Online]. Available: http://www.mdpi.com/1424-8220/18/11/3720

[20] J. Burgués, V. Hernández, A. Lilienthal, and S. Marco, "Smelling Nano Aerial Vehicle for Gas Source Localization and Mapping," *Sensors*, vol. 19, no. 3, p. 478, Jan. 2019, number: 3. [Online]. Available: https://www.mdpi.com/1424-8220/19/3/478

[21] E. Kuantama, R. Tarca, S. Dzitac, I. Dzitac, T. Vesselenyi, and I. Tarca, "The Design and Experimental Development of Air Scanning Using a Sniffer Quadcopter," *Sensors*, vol. 19, no. 18, p. 3849, Sept. 2019, number: 18. [Online]. Available: https://www.mdpi.com/1424-8220/19/18/3849

[22] J. Burgués, V. Hernández, A. J. Lilienthal, and S. Marco, "Gas distribution mapping and source localization using a 3D grid of metal oxide semiconductor sensors," *Sensors and Actuators B: Chemical*, vol. 304, p. 127309, Feb. 2020. [Online]. Available: https://linkinghub.elsevier.com/retrieve/pii/S0925400519315084

[23] G. Korotcenkov and B. K. Cho, "Instability of metal oxide-based conductometric gas sensors and approaches to stability improvement (short survey)," *Sensors and Actuators B: Chemical*, vol. 156, no. 2, pp. 527–538, Aug. 2011. [Online]. Available: https://www.sciencedirect.com/science/article/pii/S0925400511001353

[24] A. Hayes, A. Martinoli, and R. Goodman, "Distributed odor source localization," *IEEE Sensors Journal*, vol. 2, no. 3, pp. 260–271, June 2002, number: 3. [Online]. Available: http://ieeexplore.ieee.org/document/1021067/

[25] J.-G. Li, Q.-H. Meng, Y. Wang, and M. Zeng, "Odor source localization using a mobile robot in outdoor airflow environments with a particle filter algorithm," *Autonomous Robots*, vol. 30, no. 3, pp. 281–292, Apr. 2011. [Online]. Available: http://link.springer.com/10.1007/s10514-011-9219-2

[26] M. Schmuker, V. Bahr, and R. Huerta, "Exploiting plume structure to decode gas source distance using metal-oxide gas sensors," *Sensors and Actuators B: Chemical*, vol. 235, pp. 636–646, 2016. [Online]. Available: https://www.sciencedirect.com/science/article/pii/S0925400516307833